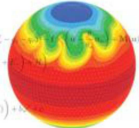


A finite-volume module for the IFS

Christian Kühnlein, Piotr Smolarkiewicz, Sylvie Malardel

$$\begin{aligned}\frac{\partial \mathcal{G}_P \rho}{\partial t} + \nabla \cdot (\mathbf{v} \mathcal{G}_P \rho) &= 0 \\ \frac{\partial \mathcal{G}_P m}{\partial t} + \nabla \cdot (\mathbf{v} \mathcal{G}_P m) &= \mathcal{G}_P \left(-\theta_L \tilde{\mathbf{G}}^T \nabla v' - \frac{H}{R_e} (b' + \theta_w (m'_w - \langle m'_w \rangle)) - \nabla \cdot (\mathbf{v} \mathcal{G}_P m') + M(u) + D \right) \\ \frac{\partial \mathcal{G}_P b'}{\partial t} + \nabla \cdot (\mathbf{v} \mathcal{G}_P b') &= \mathcal{G}_P \left(-\tilde{\mathbf{G}}^T u \cdot \nabla R_e - \frac{L}{c_P \pi} \left(\frac{\Delta \eta_{12}}{\Delta t} + \frac{\Delta \eta_{21}}{\Delta t} \right) + \nabla \cdot (\mathbf{v} \mathcal{G}_P b) \right) \\ \frac{\partial \mathcal{G}_P \rho_{12}}{\partial t} + \nabla \cdot (\mathbf{v} \mathcal{G}_P \rho_{12}) &= \mathcal{G}_P R^{12} \\ \frac{\partial \mathcal{G}_P \rho_{21}}{\partial t} + \nabla \cdot (\mathbf{v} \mathcal{G}_P \rho_{21}) &= \mathcal{G}_P R^{21} \\ \frac{\partial \mathcal{G}_P \rho'_w}{\partial t} + \nabla \cdot (\mathbf{v} \mathcal{G}_P \rho'_w) &= \mathcal{G}_P \sum_{j=1}^3 \left(\frac{n_j}{C} \nabla \cdot \hat{\zeta}_j (\hat{v} - \tilde{\mathbf{G}}^T \mathbf{C} \nabla v') \right) + \delta \omega_w\end{aligned}$$


Smolarkiewicz P. K., Deconinck W., Hamrud M., Kühnlein C., Mozdzynski G., Szmelter J., Wedi, N. P.: A finite-volume module for simulating global all-scale atmospheric flows. J. Comput. Phys., 2016



Operational configuration of IFS at ECMWF

Current operational configuration of the Integrated Forecasting System (IFS):

- hydrostatic primitive equations (nonhydrostatic option available; see Benard et al. 2014)
- hybrid $\eta - p$ vertical coordinate (Simmons and Burridge, 1982)
- spherical harmonics discretisation in horizontal (Wedi et al., 2013)
- finite-element discretisation in vertical (Untch and Hortal, 2004)
- semi-implicit semi-Lagrangian (SISL) integration scheme (Temperton et al. 2001, Diamantakis 2014)
- cubic-octahedral (" T_{co} ") grid (Wedi, 2014, Malardel et al. 2016, Smolarkiewicz et al. 2016)
- HRES: $T_{co}1279$ (O1280) with $\Delta_h \sim 9$ km and 137 vertical levels
- ENS (1+50 perturbed members): $T_{co}639$ (O640) with $\Delta_h \sim 16$ km and 91 vertical levels



*IFS parallel decomposition
with 1600 MPI tasks*

- in the near future, spectral approach (as in IFS) is assumed to remain highly competitive in terms of time-to-solution
- however, uncertainties concerning scalability/efficiency of spectral discretisation with respect to future HPC architectures

Operational configuration of IFS at ECMWF

Current operational configuration of the Integrated Forecasting System (IFS):

- hydrostatic primitive equations (nonhydrostatic option available; see Benard et al. 2014)
- hybrid $\eta - p$ vertical coordinate (Simmons and Burridge, 1982)
- spherical harmonics discretisation in horizontal (Wedi et al., 2013)
- finite-element discretisation in vertical (Untch and Hortal, 2004)
- semi-implicit semi-Lagrangian (SISL) integration scheme (Temperton et al. 2001, Diamantakis 2014)
- cubic-octahedral (" T_{co} ") grid (Wedi, 2014, Malardel et al. 2016, Smolarkiewicz et al. 2016)
- HRES: $T_{co}1279$ (O1280) with $\Delta_h \sim 9$ km and 137 vertical levels
- ENS (1+50 perturbed members): $T_{co}639$ (O640) with $\Delta_h \sim 16$ km and 91 vertical levels



*IFS parallel decomposition
with 1600 MPI tasks*

- in the near future, spectral approach (as in IFS) is assumed to remain highly competitive in terms of time-to-solution
- however, uncertainties concerning scalability/efficiency of spectral discretisation with respect to future HPC architectures

Operational configuration of IFS at ECMWF

Current operational configuration of the Integrated Forecasting System (IFS):

- hydrostatic primitive equations (nonhydrostatic option available; see Benard et al. 2014)
- hybrid $\eta - p$ vertical coordinate (Simmons and Burridge, 1982)
- spherical harmonics discretisation in horizontal (Wedi et al., 2013)
- finite-element discretisation in vertical (Untch and Hortal, 2004)
- semi-implicit semi-Lagrangian (SISL) integration scheme (Temperton et al. 2001, Diamantakis 2014)
- cubic-octahedral (" T_{co} ") grid (Wedi, 2014, Malardel et al. 2016, Smolarkiewicz et al. 2016)
- HRES: $T_{co}1279$ (O1280) with $\Delta_h \sim 9$ km and 137 vertical levels
- ENS (1+50 perturbed members): $T_{co}639$ (O640) with $\Delta_h \sim 16$ km and 91 vertical levels



*IFS parallel decomposition
with 1600 MPI tasks*

- in the near future, spectral approach (as in IFS) is assumed to remain highly competitive in terms of time-to-solution
- however, uncertainties concerning scalability/efficiency of spectral discretisation with respect to future HPC architectures



European Research Council

Established by the European Commission

Supporting top researchers
from anywhere in the world

⇒ PantaRhei project at ECMWF: prepare the mathematical-numerical technology
for future cloud-resolving earth-system

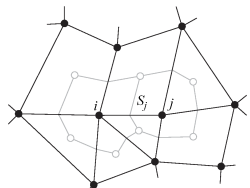
Supplement IFS with a finite-volume module (FVM) that introduces:

- finite-volume (→ compact stencil, conservative)
- all-scale compressible Euler equations
- flexible meshes
- steep orography capability



FVM formulation – key features

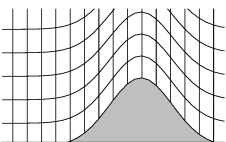
- compressible Euler equations in geospherical coordinates
- generalised curvilinear coordinates (Prusa & Smolarkiewicz JCP 2003; Wedi & Smolarkiewicz JCP 2003; Kühnlein et al. JCP 2012)
- fully unstructured edge-based finite-volume discretisation in horizontal (Szmelter & Smolarkiewicz, JCP 2010)
- structured flux-form finite-difference discretisation in vertical (Smolarkiewicz et al. JCP 2016)
- all prognostic variables are co-located
- two-time-level semi-implicit integration scheme with 3d implicit acoustic, buoyant and rotational modes (Smolarkiewicz, Kühnlein, Wedi JCP 2014)
- preconditioned generalised conjugate residual iterative solver for elliptic problems arising in semi-implicit integration schemes
- Eulerian advection with non-oscillatory forward-in-time MPDATA scheme (Smolarkiewicz and Szmelter JCP 2005; Kühnlein and Smolarkiewicz, prep. to JCP)



median-dual finite-volume approach

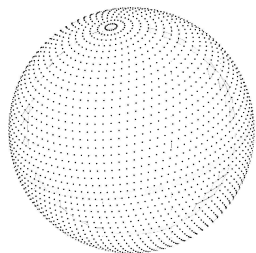
$$\int_{\Omega} \nabla \cdot \mathbf{A} = \int_{\partial\Omega} \mathbf{A} \cdot \mathbf{n} = \frac{1}{V_i} \sum_{j=1}^{l(i)} A_j^\perp S_j$$

dual volume: V_i , face area: S_j

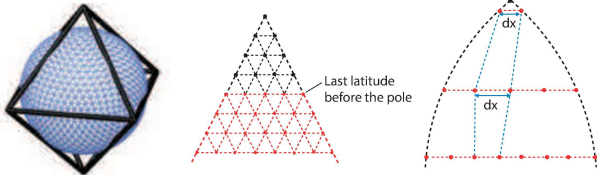


Octahedral reduced Gaussian grid

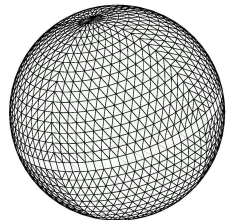
O24



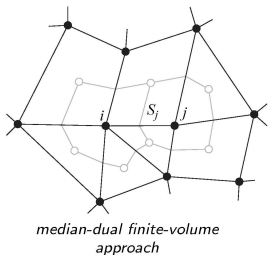
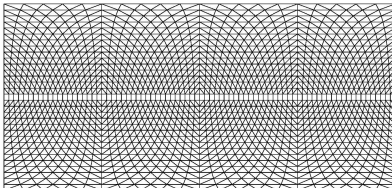
- suitable for spherical harmonics transforms applied in spectral IFS
 - Gaussian latitudes ⇒ Legendre transforms
 - uniform spacing of points along latitudes ⇒ Fourier transforms
- Notation is 'OX', for octahedral grid with X latitudes between pole and equator
- quasi-uniform resolution over the sphere
- operational at ECMWF with HRES and ENS since March 2016
- Malardel et al. ECMWF Newsletter 2016, Smolarkiewicz et al. JCP 2016



Octahedral reduced Gaussian grid



O16



- FVM develops median-dual mesh around nodes of octahedral grid
- operational spectral IFS and FVM can operate on same horizontal grid
- FVM formulation is not restricted to this grid
- Parallel data structures and mesh generator provided by Atlas (Deconinck et al., in prep. for Comput. Phys. Commun.)

$$\begin{aligned}
 & \frac{\partial \mathcal{G}\rho}{\partial t} + \nabla \cdot (\mathbf{v}\mathcal{G}\rho) = 0 \\
 \frac{\partial \rho \mathcal{G}\mathbf{u}}{\partial t} + \nabla \cdot (\mathbf{v}\rho \mathcal{G}\mathbf{u}) &= \rho \mathcal{G} \left(-\Theta_d \tilde{\mathbf{G}} \nabla \varphi' - \frac{\mathbf{g}}{\theta_a} (\theta' + \theta_a(\varepsilon q'_v - q_c - q_p)) - \mathbf{f} \times (\mathbf{u} - \Upsilon_C \mathbf{u}_a) + \mathbf{M} \right) \\
 \frac{\partial \rho \mathcal{G}\theta'}{\partial t} + \nabla \cdot (\mathbf{v}\rho \mathcal{G}\theta') &= \rho \mathcal{G} \left(-\tilde{\mathbf{G}}^T \mathbf{u} \cdot \nabla \theta_a - \frac{L\theta}{c_p T} (C_d + E_p) + \mathcal{H} \right) \\
 \varphi' &= c_p \theta_0 \left[\left(\frac{R_d}{p_0} \rho \theta (1 + q_v/\epsilon) \right)^{R_d/c_v} - \pi_a \right] \\
 \frac{\partial \rho \mathcal{G}q_v}{\partial t} + \nabla \cdot (\mathbf{v}\rho \mathcal{G}q_v) &= \rho \mathcal{G} (-C_d - E_p + D_{q_v}) \\
 \frac{\partial \rho \mathcal{G}q_c}{\partial t} + \nabla \cdot (\mathbf{v}\rho \mathcal{G}q_c) &= \rho \mathcal{G} (C_d - A_p - C_p + D_{q_c}) \\
 \frac{\partial \rho \mathcal{G}q_p}{\partial t} + \nabla \cdot (\mathbf{v}\rho \mathcal{G}q_p) &= \rho \mathcal{G} (A_p + C_p + E_p + D_{q_p}) - \nabla \cdot (\mathbf{v}_p \rho \mathcal{G}q_p)
 \end{aligned}$$

with:

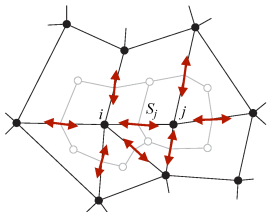
$$\Theta_d := \frac{\theta (1 + q_v/\epsilon)}{\theta_0 (1 + q_t)} \equiv \frac{\theta_d}{\theta_0} \quad \Upsilon_C \equiv \frac{\theta}{\theta_a} \quad \epsilon := \frac{R_d}{R_v} \quad \varepsilon = 1/\epsilon - 1 \quad \mathbf{v} = \tilde{\mathbf{G}}^T \mathbf{u}$$

→ "a" subscript denotes ambient state which satisfies subset of full equations, "0" subscript refers to constant reference, all primed variables are deviations with respect to the ambient state

$$(\psi' = \psi - \psi_a \quad \psi = u, v, w, \theta, \dots)$$



Finite-volume MPDATA for compressible atmospheric dynamics



Two-time-level semi-implicit solution of compressible Euler equations
(Smolarkiewicz et. al JCP 2014)

Mass continuity:

$$\rho_i^{n+1} = \mathcal{A}_i(\rho^n, (\mathbf{v}\mathcal{G})^{n+1/2}, \mathcal{G}^n, \mathcal{G}^{n+1}) \Rightarrow (\mathbf{v}^\perp \mathcal{G} \rho)^{n+1/2}$$

Conservation laws for primitive variables Ψ ($\Psi = u, v, w, \theta', \dots$):

$$\begin{aligned} \Psi_i^{n+1} &= \mathcal{A}_i(\tilde{\Psi}^n, (\mathbf{v}^\perp \mathcal{G} \rho)^{n+1/2}, (\mathcal{G} \rho)^n, (\mathcal{G} \rho)^{n+1}) + 0.5 \delta t R^\Psi|_i^{n+1} \\ &\text{with } \tilde{\Psi}^n \equiv \Psi^n + 0.5 \delta t R^\Psi|^n \end{aligned}$$

$\mathcal{A}()$ -operator is FV-MPDATA for homogeneous equation (Smolarkiewicz & Szmelter, 2005):

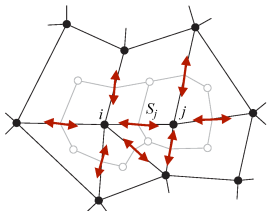
$$\frac{\partial G\psi}{\partial t} + \nabla \cdot (\mathbf{V}\psi) = 0 \quad \rightarrow \quad \psi_i^{n+1} = \psi_i^n - \frac{\delta t}{G_i V_i} \sum_{j=1}^{l(i)} F_j^\perp(\psi_i^n, \psi_j^n, V_j^\perp) S_j$$

with **normal** upwind flux: $F_j^\perp(\psi_i, \psi_j, V_j^\perp) = [V_j^\perp]^+ \psi_i + [V_j^\perp]^- \psi_j$ where $V^\perp := \mathbf{V} \cdot \mathbf{n}$

- First step is classical upwind scheme with advection of ψ by physical flow \mathbf{V}
- Error-compensative step with pseudo-velocity $\tilde{V}^\perp := -\psi^{-1} \times \text{Error}(\delta r, \delta t)$ from modified equation analysis, e.g.

$$\text{Error} = -\frac{1}{2} |V_j^\perp| \left(\frac{\partial \psi}{\partial r} \right)_{s_j}^* (r_j - r_i) + \frac{1}{2} \delta t \frac{V_j^\perp}{G_j} \{ \mathbf{V} \cdot \nabla \psi \}_{s_j}^* + \frac{1}{2} \delta t \frac{V_j^\perp}{G_j} \{ \psi (\nabla \cdot \mathbf{V}) \}_{s_j}^* + \text{HOT}$$





Two-time-level semi-implicit solution of compressible Euler equations
(Smolarkiewicz et. al JCP 2014)

Mass continuity:

$$\rho_i^{n+1} = \mathcal{A}_i(\rho^n, (\mathbf{v}\mathcal{G})^{n+1/2}, \mathcal{G}^n, \mathcal{G}^{n+1}) \Rightarrow (\mathbf{v}^\perp \mathcal{G} \rho)^{n+1/2}$$

Conservation laws for primitive variables Ψ ($\Psi = u, v, w, \theta', \dots$):

$$\begin{aligned} \Psi_i^{n+1} &= \mathcal{A}_i(\tilde{\Psi}^n, (\mathbf{v}^\perp \mathcal{G} \rho)^{n+1/2}, (\mathcal{G} \rho)^n, (\mathcal{G} \rho)^{n+1}) + 0.5 \delta t R^\Psi |_i^{n+1} \\ &\text{with } \tilde{\Psi}^n \equiv \Psi^n + 0.5 \delta t R^\Psi |^n \end{aligned}$$

$\mathcal{A}()$ -operator is FV-MPDATA for homogeneous equation (Smolarkiewicz & Szmelter, 2005):

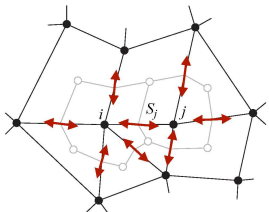
$$\frac{\partial G\psi}{\partial t} + \nabla \cdot (\mathbf{V}\psi) = 0 \quad \rightarrow \quad \psi_i^{n+1} = \psi_i^n - \frac{\delta t}{G_i \mathcal{V}_i} \sum_{j=1}^{l(i)} F_j^\perp (\psi_i^n, \psi_j^n, V_j^\perp) S_j$$

with **normal** upwind flux: $F_j^\perp (\psi_i, \psi_j, V_j^\perp) = [V_j^\perp]^+ \psi_i + [V_j^\perp]^- \psi_j$ where $V^\perp := \mathbf{V} \cdot \mathbf{n}$

- First step is classical upwind scheme with advection of ψ by physical flow \mathbf{V}
- Error-compensative step with pseudo-velocity $\tilde{V}^\perp := -\psi^{-1} \times \text{Error}(\delta r, \delta t)$ from modified equation analysis, e.g.

$$\text{Error} = -\frac{1}{2} |V_j^\perp| \left(\frac{\partial \psi}{\partial r} \right)_{s_j}^* (r_j - r_i) + \frac{1}{2} \delta t \frac{V_j^\perp}{G_j} \{ \mathbf{V} \cdot \nabla \psi \}_{s_j}^* + \frac{1}{2} \delta t \frac{V_j^\perp}{G_j} \{ \psi (\nabla \cdot \mathbf{V}) \}_{s_j}^* + \text{HOT}$$





Two-time-level semi-implicit solution of compressible Euler equations
(Smolarkiewicz et. al JCP 2014)

Mass continuity:

$$\rho_i^{n+1} = \mathcal{A}_i(\rho^n, (\mathbf{v}\mathcal{G})^{n+1/2}, \mathcal{G}^n, \mathcal{G}^{n+1}) \Rightarrow (\mathbf{v}^\perp \mathcal{G} \rho)^{n+1/2}$$

Conservation laws for primitive variables Ψ ($\Psi = u, v, w, \theta', \dots$):

$$\Psi_i^{n+1} = \mathcal{A}_i(\tilde{\Psi}^n, (\mathbf{v}^\perp \mathcal{G} \rho)^{n+1/2}, (\mathcal{G} \rho)^n, (\mathcal{G} \rho)^{n+1}) + 0.5 \delta t R^\Psi |_i^{n+1}$$

with $\tilde{\Psi}^n \equiv \Psi^n + 0.5 \delta t R^\Psi |_i^n$

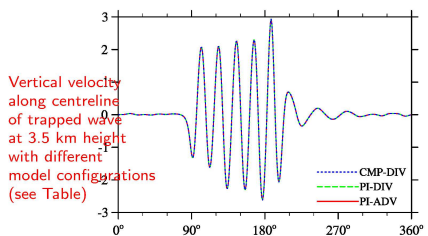
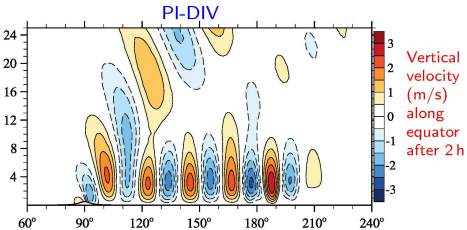
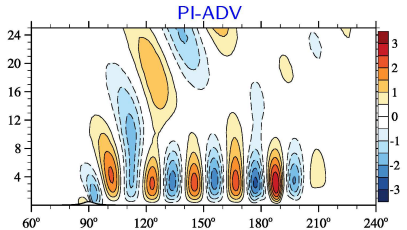
FV-MPDATA solely using face-normal vector components (Kühnlein and Smolarkiewicz, in prep. for JCP):

$$\text{Error} = -\frac{1}{2} |V_j^\perp| \left(\frac{\partial \psi}{\partial r} \right)_{s_j}^* (r_j - r_i) + \frac{1}{2} \delta t \frac{V_j^\perp}{G_j} \{ \nabla \cdot (\mathbf{v} \psi) \}_{s_j}^* + \text{HOT}$$

Gauss-divergence theorem: $\int_{\Omega} \nabla \cdot \mathbf{A} = \int_{\partial \Omega} \mathbf{A} \cdot \mathbf{n} = \frac{1}{V_i} \sum_{j=1}^{l(i)} A_j^\perp S_j$

Finite-volume MPDATA for compressible atmospheric dynamics

Orographically-forced internal gravity waves in sheared ambient flow on small planet (Keller 1994, Wedi & Smolarkiewicz 2009) with octahedral grid O90:



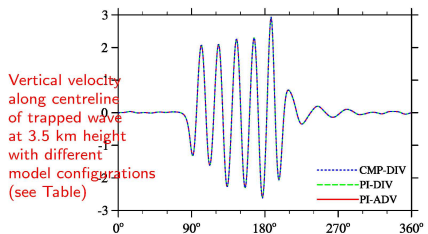
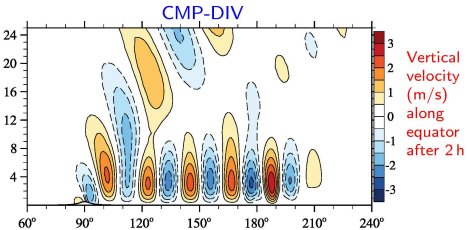
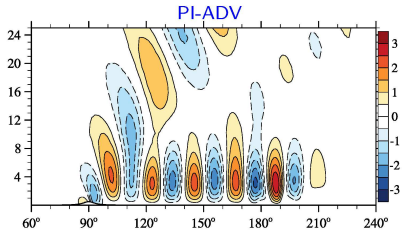
Simulation	Equations	FV-MPDATA
PI-ADV	pseudo-incompressible	established form
PI-DIV	pseudo-incompressible	advanced form
CMP-DIV	fully compressible Euler	advanced form

⇒ Proposed FV-MPDATA reproduces reference results of established formulation and enables effective semi-implicit integration of compressible Euler equations on arbitrary meshes



Finite-volume MPDATA for compressible atmospheric dynamics

Orographically-forced internal gravity waves in sheared ambient flow on small planet (Keller 1994, Wedi & Smolarkiewicz 2009) with octahedral grid O90:



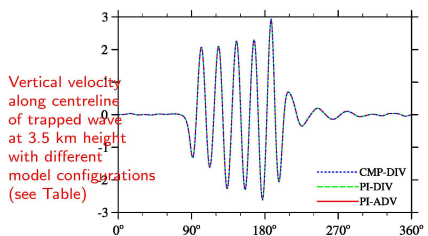
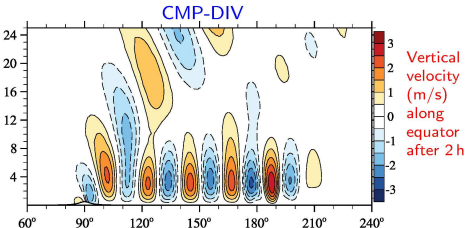
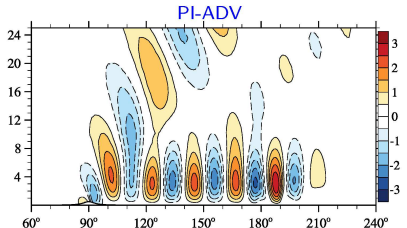
Simulation	Equations	FV-MPDATA
PI-ADV	pseudo-incompressible	established form
PI-DIV	pseudo-incompressible	advanced form
CMP-DIV	fully compressible Euler	advanced form

⇒ Proposed FV-MPDATA reproduces reference results of established formulation and enables effective semi-implicit integration of compressible Euler equations on arbitrary meshes



Finite-volume MPDATA for compressible atmospheric dynamics

Orographically-forced internal gravity waves in sheared ambient flow on small planet (Keller 1994, Wedi & Smolarkiewicz 2009) with octahedral grid O90:

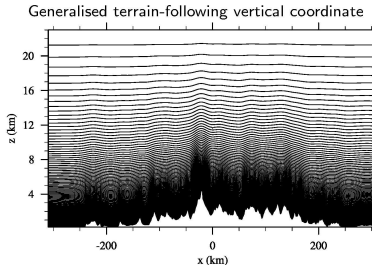


Simulation	Equations	FV-MPDATA
PI-ADV	pseudo-incompressible	established form
PI-DIV	pseudo-incompressible	advanced form
CMP-DIV	fully compressible Euler	advanced form

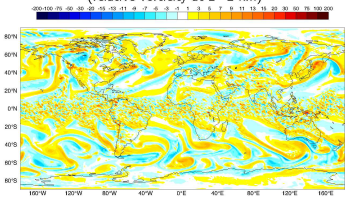
⇒ Proposed FV-MPDATA reproduces reference results of established formulation and enables effective semi-implicit integration of compressible Euler equations on arbitrary meshes



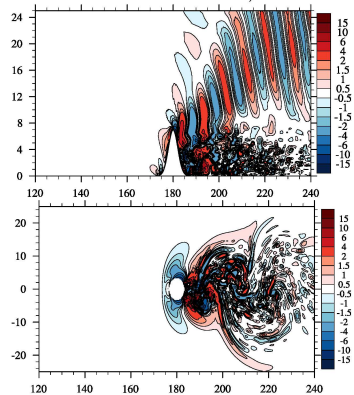
Vertical discretisation and incorporation of orography in FVM



Held-Suarez benchmark N640 (16 km) with realistic IFS orography at day 90
(relative vorticity at $z=2$ km)



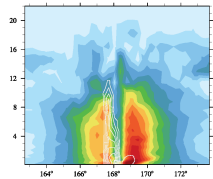
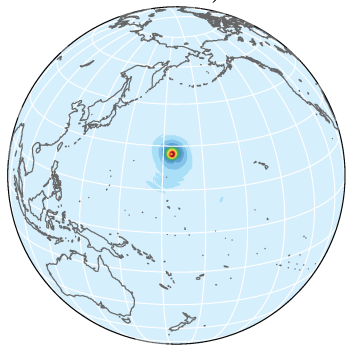
stratified flow past steep orography with maximum slope $\sim 70^\circ$ on small planet
(vertical velocity in m/s, lon-height section at lat=0,
lon-lat section at $z=2$ km)



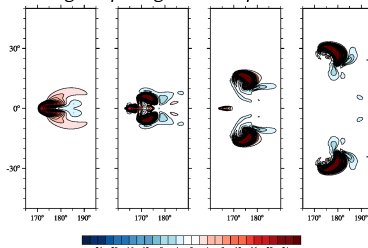
⇒ robust and efficient handling of steep orography

Dynamical Core Model Intercomparison Project 2016

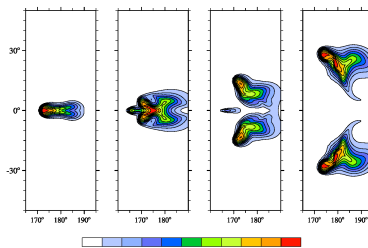
Tropical cyclone with FVM at day 10 ($\Delta_h = 0.25^\circ$):



Supercell evolution (0.5, 1, 1.5, 2h) with FVM at 500 m grid spacing on small planet:



Vertical velocity
(m/s)
at 5 km



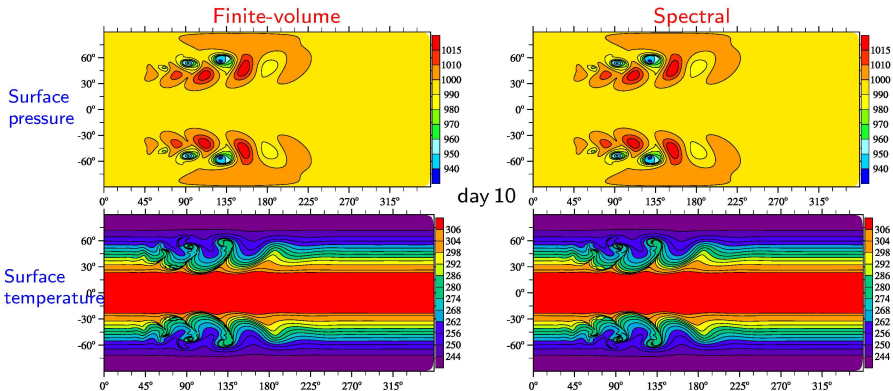
Rainwater
(g/kg)
at 5 km

→ FVM with simplified cloud microphysics and PBL parametrisations



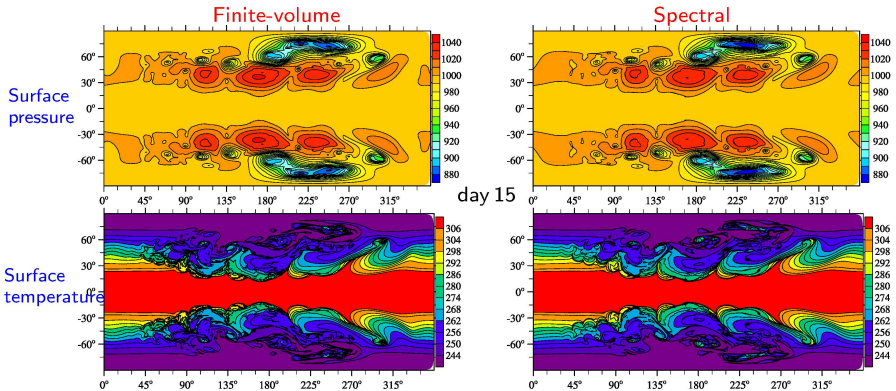
Finite-volume versus spectral solutions in the IFS

Dry baroclinic instability, FVM (O640) versus the spectral IFS ($T_{co}639$):



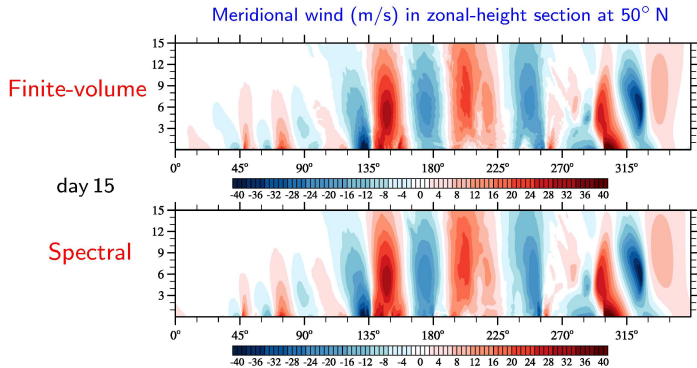
Finite-volume versus spectral solutions in the IFS

Dry baroclinic instability, FVM (O640) versus the spectral IFS ($T_{co}639$):



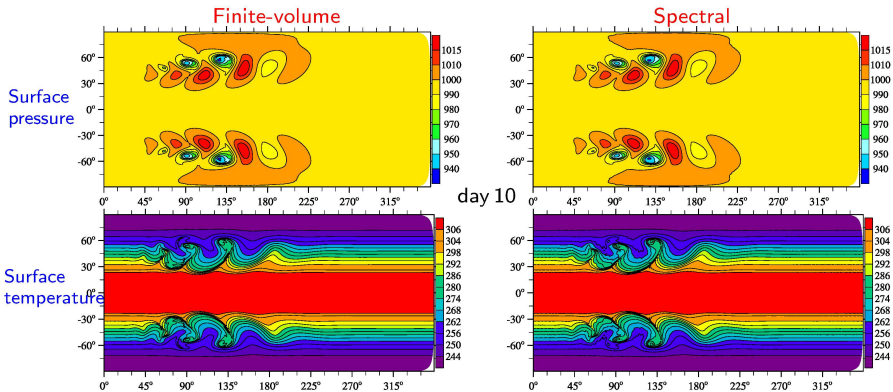
Finite-volume versus spectral solutions in the IFS

Dry baroclinic instability, FVM (O640) versus the spectral IFS ($T_{co}639$):



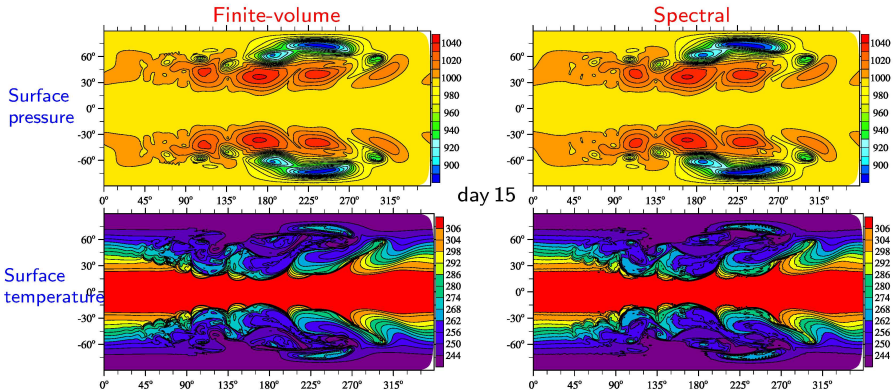
Finite-volume versus spectral solutions in the IFS

Dry baroclinic instability, FVM (O160) versus the spectral IFS ($T_{co}159$):

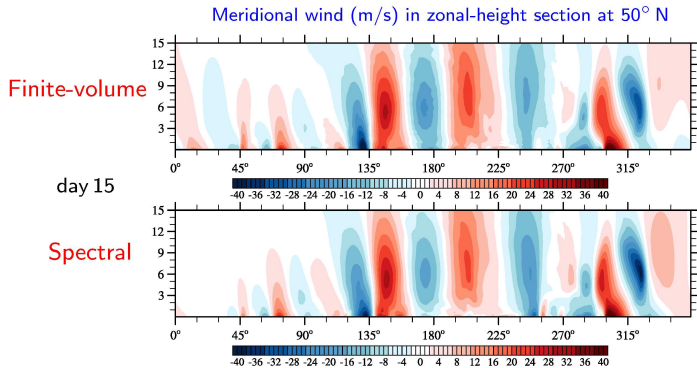


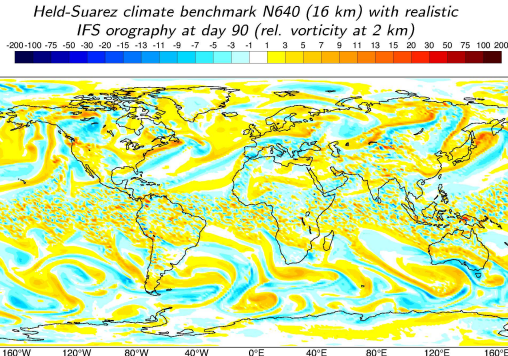
Finite-volume versus spectral solutions in the IFS

Dry baroclinic instability, FVM (O160) versus the spectral IFS ($T_{co}159$):



Dry baroclinic instability, FVM (O160) versus the spectral IFS ($T_{co}159$):





Outlook:

- Efficiency at high resolution and extreme scaling (\rightarrow ESCAPE)
- Comprehensive comparison of FVM with spectral IFS
- Towards more realism (Initial conditions, parametrisations,...)

TECHNICAL MEMORANDUM

760

The modelling infrastructure of the Integrated Forecasting System: Recent advances and future challenges

N.P. Wedi, P. Bauer, W. Deconinck, M. Diamantakis, M. Hamrud, C. Kühnlein, S. Malardel, K. Mogensen, G. Mozdzynski, P.K. Smolarkiewicz

Research Department

November 2015

Special topic paper presented at the 44th session of ECMWF's Scientific Advisory Committee, Reading, UK

The paper has not been published and should be regarded as an Internal Report from ECMWF.
Reproduction to quote from it should be obtained from the ECMWF.



European Centre for Medium-Range Weather Forecasts
Europäisches Zentrum für mittelfristige Wettervorhersage
Centre européen pour les prévisions météorologiques à moyen

Journal of Computational Physics 274 (2014) 207–238

Contents lists available at ScienceDirect



Journal of Computational Physics

www.elsevier.com/locate/jcp



A finite-volume module for simulating global all-scale atmospheric flows

Piotr K. Smolarkiewicz^{a,*}, Willem Deconinck^a, Mars Hamrud^b, Christian Kühnlein^c, George Mozdzynski^c, Joanna Szmelcer^b, Nils P. Wedi^a

^a European Centre for Medium-Range Weather Forecasts, Reading, RG2 9AX, UK

^b Loughborough University, Loughborough LE11 3TU, UK

ARTICLE INFO

Received 15 August 2013
Received in revised form 7 March 2014
Accepted 5 March 2014
Available online 10 March 2014

Keywords: Atmospheric models
Spectral transform modeling
Non-circularity forward-in-time schemes
Gravity waves
Numerical weather prediction

ABSTRACT

The paper documents the development of a global hydrostatic finite-volume module designed specifically at the European Centre for Medium-Range Weather Forecasts (ECMWF) need. The module adheres to NWP standards, with formulation of the governing equations based on the classical meteorological latitude-longitude spherical framework. In the horizontal, a hexagonal unstructured mesh with finite-volumes built about the refined Gaussian grid of the existing NWP model encompasses the resolution switch in the polar regions, while maintaining the same grid. All dependent variables are stored according to specific standards and grid-point relations at the same physical locations. In the vertical, a uniform time-difference discretization facilitates the solution of elliptic problems in thin spherical shells, while the physics of the physical vertical coordinate is designed to generate continuous transitions between computational and physical vertical coordinates. The module uses spectral-transform spatial discretization for advection, but includes reduced wavenumber (PW) as an option. Furthermore, it employs semi-implicit forward-in-time integration of the governing PW system, akin to but more general than those used in the NWP model. The module shares the equal temporal parameterization scheme of the NWP model, with multiple layers of parallel hydrostatic MPI tasks and OpenMP threads. The efficacy of the developed hydrostatic module is illustrated with benchmarks of idealized global weather.

© 2014 Elsevier Inc. All rights reserved.

1. Introduction

Numerical weather prediction (NWP) has achieved high proficiency over the past 30 years. This owes much to advancements in computer hardware, observational networks and data assimilation techniques as well as numerical methods for integrating hydrostatic primitive equations (HPE), the particular numerical approach embraced widely by NWP combines semi-implicit time stepping with semi-Lagrangian advection (SLA) and with spectral-transform spatial discretisation of the governing HPE [46]. The SLA time stepping enables integrations with Courant numbers of the fluid flow and wave motions much larger than unity, whereas the spectral-transform discretisation facilitates the efficient solution of elliptic equations induced by the SLA approach. Moreover, it circumvents the computational expense of the latitude-longitude (lat-lon) co-

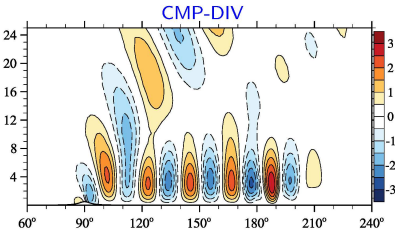
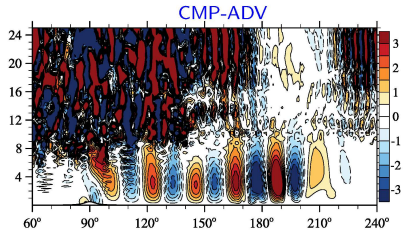
* Corresponding author.
E-mail address: smola@ecmwf.int (P.K. Smolarkiewicz).

<http://dx.doi.org/10.1016/j.jcp.2014.03.015>
0021-9604/\$ – see front matter © 2014 Elsevier Inc. All rights reserved.



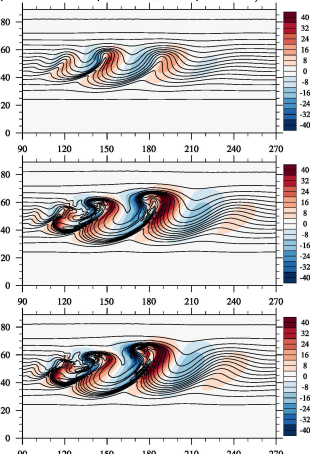
Finite-volume MPDATA for compressible atmospheric dynamics

Orographically-forced internal gravity waves in sheared ambient flow on small planet (Keller 1994, Wedi & Smolarkiewicz 2009) with octahedral grid O90:



Options for 3D governing equations in FVM

Baroclinic instability (Jablonowski and Williamson, 2006) with FVM (from top: anelastic, pseudo-incompressible, compressible)



→ Generic nonhydrostatic formulation with consistent options:

- ★ fully compressible Euler equations (default)
- ★ pseudo-incompressible (Durran, JAS 1989)
- ★ anelastic (Lipps and Hemler, JAS 1982)

$$\frac{\partial \mathcal{G}\varrho}{\partial t} + \nabla \cdot (\mathbf{v}\mathcal{G}\varrho) = 0$$
$$\frac{\partial \mathcal{G}\varrho\mathbf{u}}{\partial t} + \nabla \cdot (\mathbf{v}\mathcal{G}\varrho\mathbf{u}) = -\mathcal{G}\varrho \left(\Theta \tilde{\mathbf{G}} \nabla \varphi' + \mathbf{g} \Upsilon_B \frac{\theta'}{\theta_b} + \mathbf{f} \times (\mathbf{u} - \Upsilon_C \mathbf{u}_a) + \mathbf{M} \right)$$
$$\frac{\partial \mathcal{G}\varrho\theta'}{\partial t} + \nabla \cdot (\mathbf{v}\mathcal{G}\varrho\theta') = -\mathcal{G}\varrho \left(\tilde{\mathbf{G}}^T \mathbf{u} \cdot \nabla \theta_a \right)$$

with optional coefficients:

$$\varrho := [\rho(\mathbf{x}, t), \rho_b \frac{\theta_b(z)}{\theta_0}, \rho_b(z)] , \quad \varphi' := [c_p \theta_0 \pi', c_p \theta_0 \pi', c_p \theta_b \pi']$$
$$\Theta := \left[\frac{\theta}{\theta_0}, \frac{\theta}{\theta_0}, 1 \right] , \quad \Upsilon_B := \left[\frac{\theta_b(z)}{\theta_a(\mathbf{x})}, \frac{\theta_b(z)}{\theta_a(\mathbf{x})}, 1 \right] , \quad \Upsilon_C := \left[\frac{\theta}{\theta_a(\mathbf{x})}, \frac{\theta}{\theta_a(\mathbf{x})}, 1 \right]$$

